

pubs.acs.org/ac Article

Low-Cost High-Pressure Clinical-Scale 50% Parahydrogen Generator Using Liquid Nitrogen at 77 K

Benjamin Chapman, Baptiste Joalland, Collier Meersman, Jessica Ettedgui, Rolf E. Swenson, Murali C. Krishna, Panayiotis Nikolaou, Kirill V. Kovtunov, Oleg G. Salnikov, Igor V. Koptyug, Max E. Gemeinhardt, Boyd M. Goodson, Roman V. Shchepin, and Eduard Y. Chekmenev*



Cite This: https://doi.org/10.1021/acs.analchem.1c00716

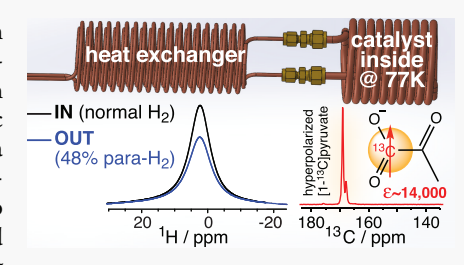


ACCESS

Metrics & More

Article Recommendations

ABSTRACT: We report on a robust and low-cost parahydrogen generator design employing liquid nitrogen as a coolant. The core of the generator consists of catalyst-filled spiral copper tubing, which can be pressurized to 35 atm. Parahydrogen fraction >48% was obtained at 77 K with three nearly identical generators using paramagnetic hydrated iron oxide catalysts. Parahydrogen quantification was performed on the fly via benchtop NMR spectroscopy to monitor the signal from residual orthohydrogen—parahydrogen is NMR silent. This real-time quantification approach was also used to evaluate catalyst activation at up to 1.0 standard liter per minute flow rate. The reported inexpensive device can be employed for a wide range of studies employing



parahydrogen as a source of nuclear spin hyperpolarization. To this end, we demonstrate the utility of this parahydrogen generator for hyperpolarization of concentrated sodium [1-¹³C]pyruvate, a metabolic contrast agent under investigation in numerous clinical trials. The reported pilot optimization of SABRE-SHEATH (signal amplification by reversible exchange—shield enables alignment transfer to heteronuclei) hyperpolarization yielded ¹³C signal enhancement of over 14,000-fold at a clinically relevant magnetic field of 1 T corresponding to approximately 1.2% ¹³C polarization—if near 100% parahydrogen would have been employed, the reported value would be tripled to ¹³C polarization of 3.5%.

INTRODUCTION

NMR hyperpolarization techniques enhance the detection sensitivity of NMR spectroscopy and imaging by several orders of magnitude. These tremendous gains in detection sensitivity enable new applications, including molecular imaging of exogenous contrast agents. The nuclear spins of these new contrast agents are hyperpolarized (HP) using a wide range of techniques. Some hyperpolarization techniques have been successfully employed in clinical trials. Despite the major successes in clinical research, none of these methods have enjoyed widespread or routine clinical use so far, in part because of high instrumentation cost and low hyperpolarization throughput.

Parahydrogen-induced polarization (PHIP) is a simple, fast, and low-cost hyperpolarization approach ^{15,16} that has the potential to revolutionize the production of HP contrast agents for clinical use. Canonical PHIP requires pairwise parahydrogen (p-H₂) addition to an unsaturated molecular substrate. ^{17,18} More recently, the nonhydrogenative variant called signal amplification by reversible exchange (SABRE) has emerged: ^{19,20} the latter method employs chemical exchange of p-H₂ and to-be-hyperpolarized substrates on metal complexes. ^{21,22} Both PHIP and SABRE approaches have produced a range of HP contrast agents with some validation success in

cellular and preclinical models $^{23-29}$ as also described in recent reviews. 10,30,31

Parahydrogen, employed as the source of nuclear spin order in PHIP, 15,32,33 is produced by transient exposure of normal dihydrogen gas (with its ambient 1:3 para-to-ortho-state distribution) to a low temperature. $^{26,34-38}$ Because p-H₂ is a lower energy state, the equilibrium shifts to the para-state at sufficiently low temperatures; 39 nearly 100% p-H₂ can be obtained at ≤ 20 K. 2,40 When pure p-H₂ is employed for PHIP, near-unity proton polarization can be unlocked after the magnetic equivalence of the nascent p-H₂-derived protons is broken. 15,17,41 Moreover, in both hydrogenative PHIP and its nonhydrogenative variant SABRE, it has been demonstrated that the polarization of nascent p-H₂-derived protons can be transferred via the network of spin—spin couplings to other spin-1/2 nuclei including 13 C, $^{24,42-45}$ 15 N, $^{46-48}$ 14 H, 21 31 P, 49 19 F, 50,51 and so forth. 52 Nuclear spin polarization (*P*) values in

Received: February 16, 2021 Accepted: May 27, 2021



excess of 50% have been demonstrated^{53–55} when polarization transfer is optimized using pure p-H₂ gas.

Once one has a supply of p-H2 in hand, the remaining hardware required to accomplish polarization transfer in PHIP and SABRE is relatively straightforward and low-cost (e.g., approximately \$10k for a setup employing a mass-flow controller and mu-metal shields for SABRE⁵⁶ or PHIP field cycling studies⁵⁷ at micro-tesla fields) because no cryogenic or high-field hardware is required. However, the ostensible need for pure p-H₂ would require the use of cryogenic equipment in the range of \$50,000-125,000 (e.g., Bruker or ARS generators), 26,29,34,36,58 representing a substantial investment and a barrier for those working in (or desiring to enter) the field of p-H2-based hyperpolarization. Moreover, the quantification of the p-H2 fraction is often required to ensure reproducible results in PHIP and SABRE. In the NMR hyperpolarization community, the measurement is typically performed using high-field NMR spectroscopic quantification of the residual orthohydrogen fraction—because p-H₂ is NMR silent⁵⁹ —although other methods have been demonstrated.^{60–62} Once created, the p-H₂ gas can then be stored in pressurized aluminum cylinders for weeks. 34,36,63 The requirement of a high-field NMR spectrometer adds additional complexity and cost to the infrastructure for the robust and reproducible operation of a p-H2-based hyperpolarization facility. As an alternative, we have recently demonstrated that the residual orthohydrogen fraction in near 100% p-H2 gas can be monitored in real-time using low-field benchtop NMR spectroscopy.⁶⁴ Benchtop NMR spectrometers have a substantially lower cost than high-field NMR devices; they are also portable, have a small footprint, require no cryogens to operate, and are increasingly becoming a standard "workhorse" in routine hyperpolarization studies.⁶

To mitigate the cost and complexity of cryogenic hardware, p-H₂ production can be conducted at liquid N₂ temperature (ca. 77 K at 1 atm) resulting in an approximately 50% p-H₂ fraction. Moreover, liquid He can also be employed as a chilling source resulting in a 97.5% p-H₂ fraction. The key disadvantage of using 50% (vs near 100%) p-H₂ is the reduction of the resulting hyperpolarization effect by a factor of ~3. Such substantial polarization decrease can be unforgiving for many signal-to-noise ratio-challenged applications, for example, most notably *in vivo* studies. However, many other applications—including the development phase of PHIP-and SABRE-based contrast agents—can be accomplished with this "lower" p-H₂ grade, which is much easier and cheaper to achieve in practice. $^{69-71}$

Several parahydrogen converter/generator designs employing a wide range of ortho-to-para conversion catalysts have been reported for operation at liquid N_2 temperature. $^{38,62,71-73}$ Moreover, very recently, a liquid He-based system has been employed in the production of nearly pure p-H₂ using an inexpensive design (\$1,200 in parts), 63 although the design relies on liquid He (which may impose a substantial additional running cost and infrastructure), which requires a \sim 90 min cool-down time and has limited production capacity at maximum specs [200 standard cubic centimeters per minute (sccm)].

Here, we report a robust and inexpensive design of a p- H_2 generator for operation with liquid N_2 at a tested pressure of up to 35 atm. The reported design is based on more than 10 years of experience in our laboratories. The produced compressed H_2 gas is quantified by "real-time" NMR

spectroscopy of exiting p-H₂ using a benchtop 1.4 T NMR spectrometer. The design reproducibility has been evaluated with three separately constructed devices. Moreover, we have also investigated ortho-para catalyst activation by catalyst exposure to >100 °C to achieve a production rate of 1,000 sccm with a \sim 49% p-H₂ fraction. The utility of the reported device has been tested in the feasibility demonstration of [1-13C]pyruvate hyperpolarization via SABRE, following the work of Duckett and coworkers.⁷⁴ HP [1-¹³C]pyruvate is a leading HP contrast agent employed for tracking metabolism in vivo^{7,11,12,14} and is currently being evaluated in many clinical trials and preclinical models of numerous human diseases. 13,14,75 Taken together, the reported design augmented by real-time p-H₂ quantification using benchtop NMR spectroscopy will hopefully be of interest not only to those already working in the field of NMR hyperpolarization in general (and p-H₂-based hyperpolarization in particular) but also to those seeking a low-barrier entryway into NMR hyperpolarization techniques.

MATERIALS AND METHODS

Generator Design. The core component employs copper tubing (0.25 in. outer diameter, OD; 0.03 in. wall; 0.19 in. inner diameter, ID, McMaster-Carr, P/N 5174K21; and ~115 cm length) that was filled with \sim 21 g of hydrated iron(III)oxide (Fe₂O₃·H₂O, 371254, Sigma-Aldrich, St. Louis, MO)—this material is produced as Ionex Type OP Catalyst (https://www.molecularproducts.com/products/ ionex-type-op-catalyst Molecular Products, Louisville, Colorado, USA). Prior to loading, the catalyst material was purged of microparticles by mechanical filtration via ABN strainer cone funnels with disposable 190 µm mesh https://www. amazon.com/gp/product/B01H7PEHEK/. Each funnel was filled to $\sim 1/5$ of its capacity, and the catalyst was washed with ethanol or isopropanol until the washing liquid passing through it became practically colorless. The alcohol-washed catalyst was further washed with hexane until the washing liquid became colorless as well. The washed catalyst was placed in a glass beaker and dried overnight in an oven at ~60 °C. If not removed, microparticles can degrade p-H2 generator performance if they escape downstream of the cryogenic region. The catalyst-filled copper tube was wound into a spiral with a ~2.36 in. (6 cm) OD consisting of approximately six turns [~2.75 in. (7 cm) height], Figure 1. The ends of the copper tubing were filled with glass wool to ensure the catalyst remains in the 0.25 in. copper tubing segment. Next, each end of the catalyst-filled 0.25 in. spiral tubing segment was adapted to a heat exchange 0.125 in. OD copper tubing spiral (0.03 in. wall and 0.065 in. OD, McMaster-Carr, P/N 5174K1) using brass Yor-Lok reducers (McMaster-Carr, P/N 5272K214). The two hollow spirals (~20 turns of similar diameter) made of 0.125 in. copper tubing are designed to serve two purposes. The 0.125 in. copper tubing spiral is reinforced by aluminum brackets (Figure 1) to enhance structural rigidity. In case the liquid N2 level is above the heat exchangers, the inlet heat exchanger allows for precooling of the incoming H₂ gas. Alternatively, if the liquid N2 level is below the heat exchangers, heat exchange between incoming and exiting hydrogen gas flows allows for precooling of the incoming H₂ gas while warming exiting para-enriched H2, as shown in Figure 1.

Experimental Setup for "Real-Time" Benchtop NMR Spectroscopy of Hydrogen Gas. To monitor the p-H₂

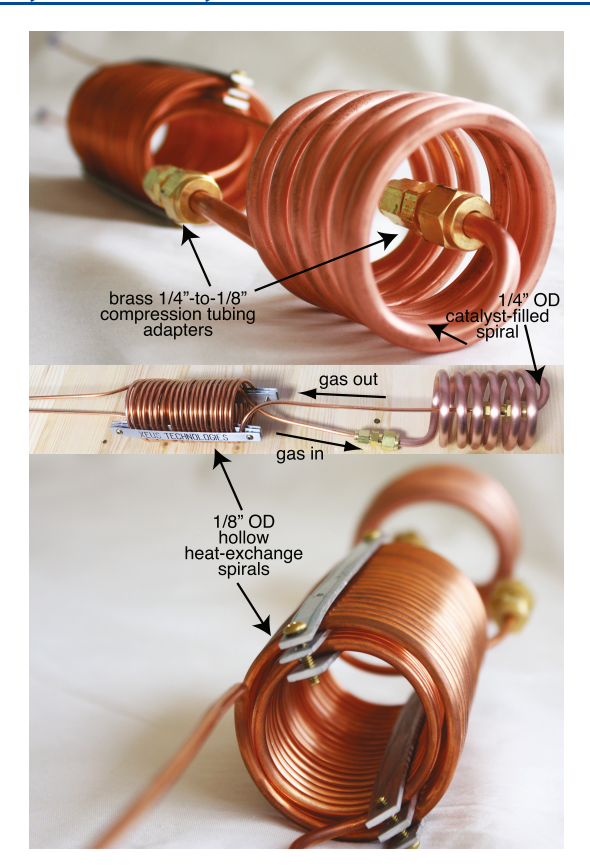


Figure 1. Annotated photographs of the p-H₂ generator device core, outlining the orientations and interfaces of key components.

enrichment on the fly, we have employed the setup described previously,⁶⁴ which was adapted for operation with the present generator, as shown in Figure 2. A high-pressure tank equipped

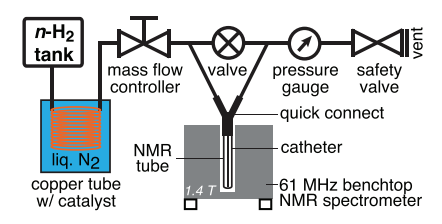


Figure 2. Experimental setup schematic employed for p- H_2 quantification studies using real-time benchtop 1.4 T NMR spectroscopy. The safety valve allows for 100 PSI overpressure, and the normal hydrogen (n- H_2) pressure of the main hydrogen tank was set to 125 PSI. Switching the valve to the "OFF" position directs hydrogen gas to an NMR tube via a 0.065 in. OD Teflon catheter.

with a dual-stage pressure regulator and containing ultrahigh-purity (>99.999%) hydrogen was connected to the input port of the generator using a Yor-Lok brass coupling. The other end of the generator was connected directly to the input of a mass flow controller (MFC; Sierra Instruments Inc., Monterey, California, USA, P/N C100L-DD-1-OV1-SV1-PV2-V1-S0, 1000 sccm model). The hydrogen tank pressure was set to $\sim\!125$ PSI. The flexible 0.125 in. copper lines allow for easy maneuvering of the generator core to insert into/remove from the liquid N_2 bath (in a Styrofoam container) or exposing the catalyst-filled section to a heat gun for catalyst activation studies (see below). Parahydrogen quantification was performed using a 1.4 T NMR spectrometer operating at 61 MHz

proton resonance frequency with gas samples at 8 atm (100 PSI overpressure) employing the following acquisition parameters: 1024 scans, 5 kHz spectral width, 52 ms acquisition time, 0.1 s repetition time, \sim 102 s total acquisition time, and 90° excitation pulse of \sim 10 μ s duration.

Parahydrogen Quantification. Parahydrogen quantification was performed using the previously described method, ⁶⁴ which was adapted for operation with the described generator. Briefly, on the day of the operation, the setup (Figure 2) was first operated at room temperature, that is, without a liquid N_2 bath. The MFC flow rate was set to 150 sccm, and the safety valve was set to 100 PSI overpressure (as confirmed by the pressure gauge, Figure 2). The valve was placed in the "OFF" position, and normal hydrogen was allowed to pass through the catheter and run through a standard 5 mm NMR tube equipped with a "Y" connector for 10 min. This "purge" stage was required to remove any residual air and moisture from the setup and to fill the NMR tube to 100 PSI overpressure with normal H_2 gas (containing 75% o- H_2).

Next, the valve is switched to the "ON" position and the gas flow is directed via bypass rather than through the NMR tube. As a result, normal hydrogen (25% para-H₂ and 75% ortho-H₂) in the tube was not flowing during NMR acquisition (instead, the flow was directed via bypass). Next, an NMR spectrum of normal H₂ gas was acquired using the acquisition parameters listed above. The signal (integrated area under the curve, AUC) was computed using SpinSolve Expert software supplied by the vendor (Magritek, New Zealand). The corresponding signal from an empty NMR tube was also acquired and subtracted from each NMR measurement to account for any background signal using the same spectral processing parameters.

The generator's catalyst-filled spiral was then submerged into a liquid N_2 bath and allowed to equilibrate at cryogenic temperature for 10 min with a continuous H_2 flow at 150 sccm. The valve was switched to the "OFF" position to direct the gas flow through the NMR tube for \sim 2 min. Next, the valve is switched "ON". As a result, para-enriched hydrogen in the tube was not flowing during NMR acquisition (instead, the flow was directed via bypass). Next, an NMR spectrum of the paraenriched H_2 gas was acquired using the acquisition parameters listed in the caption of Figure 3. The NMR signal was processed in the same fashion as for normal H_2 as described

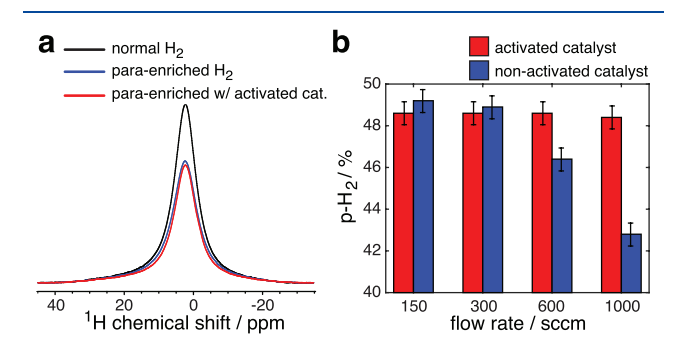


Figure 3. (a) Parahydrogen quantification using a 1.4 T NMR spectrometer operating at 61 MHz proton resonance frequency using gas samples at 8 atm (100 PSI overpressure). Acquisition parameters: 1024 scans, 5 kHz spectral width, 52 ms acquisition time, 0.1 s repetition time, \sim 102 s total acquisition time, and 90° excitation pulse (\sim 10 μ s long). (b) Dependence of the p-H₂ fraction on the flow rate for the activated and nonactivated catalyst.

above. All measurements for the p- H_2 -enriched and normal H_2 gas were repeated three times and averaged. The p- H_2 fraction (f) was computed using eq 1

$$f = 1 - \frac{3 \times S_{\text{enriched}}}{4 \times S_{\text{normal}}} \tag{1}$$

where $S_{\rm enriched}$ and $S_{\rm normal}$ are the corresponding NMR signals for p-H₂-enriched and normal (i.e., nonenriched) hydrogen gas samples, respectively. Note that multipliers 3 and 4 are used to reflect 75% o-H₂ in normal (unenriched) H₂ gas.³⁰ Three p-H₂ generators were tested for test-retest reproducibility.

Catalyst Activation. Catalyst activation was performed by heating the catalyst-containing spiral using a heat gun to >100 $^{\circ}$ C for \sim 15 min under a continuous 150 sccm flow of H₂ gas.

 13 C SABRE Hyperpolarization of [1- 13 C]pyruvate. 13 C SABRE hyperpolarization of [1-13C]pyruvate was performed using SABRE in SHield enables alignment transfer to heteronuclei (SABRE-SHEATH)^{47,48} tailored for the ¹³C nucleus^{45,76} using the DMSO-coligand approach developed by Duckett and coworkers. 74 Sodium [1-13C]-pyruvate and deuterated methanol-d₄ solvent were purchased from Sigma-Aldrich and used without any further purification. The [IrCl(COD)(IMes)] SABRE catalyst precursor was synthesized according to a literature procedure.²¹ The sample was prepared with a fixed ratio of substrate to Ir-IMes SABRE precatalyst and DMSO in 0.6 mL of methanol-d₄ in a 5 mm NMR tube with a typical ratio of substrate, catalyst (12 mM), and DMSO as 7:1:10. Ultrahigh-purity H₂ gas (Airgas) was fed into a p-H₂ generator and enriched to about 50% para-fraction using liquid N2 as described above. The p-H2 flow is directed via Polytetrafluoroethylene (PTFE) tubing using the MFC (Sierra Instruments SmartTrak 100 series) set at 80 sccm flow rate and directed to a conventional 5 mm NMR tube (Norell) to allow for p-H₂ bubbling through the sample. The entire p-H₂ line was pressurized to 40 PSI overpressure unless otherwise noted. SABRE-SHEATH requires the use of microtesla or submicrotesla magnetic fields to enable efficient polarization transfer from p-H2-derived hydrides to heteronuclei (e.g., ¹³C targeted here). In practice, these fields are achieved by attenuating the Earth's magnetic field and creating a minute magnetic field inside the shield using electromagnets. Here, magnetic fields near or below $\sim 1 \mu T$ were achieved with a home-built apparatus consisting of a solenoid coil placed inside a mu-metal shield (Magnetic Shield Corporation, model no. ZG-206). This solenoid is 41 mm in diameter: 40 mm core, 20 cm long windings with 220 turns of AWG20 (0.9 mm) Cu wire and with 220 Ω resistor in series. The solenoid coil was driven by commercial 1.5 V batteries with a variable resistance decade box in series to provide finer control of the internal magnetic field of the shield, which is monitored using a Lakeshore Cryotronics Gaussmeter (model no. 475 DSP with HMMA-2512-VR Hall probe). NMR experiments were performed using a 1 T Magritek Spinsolve benchtop NMR spectrometer. All ¹³C NMR spectra were taken without ¹H decoupling throughout the duration of the experiment. The time required to manually transfer the sample from the shield region to the magnet for low-field NMR acquisition was usually <5 s. The ¹³C signal enhancement was computed by comparing the HP signal AUC to the external 13C signal thermal signal reference (4 M sodium [1-13C]acetate) using eq

$$\varepsilon(^{13}C) = \frac{S_{HP}}{S_{REF}} \cdot \frac{C_{REF}}{C_{HP}} \cdot \frac{A_{REF}}{A_{HP}}$$
(2)

where $S_{\rm HP}$ and $S_{\rm REF}$ are $^{13}{\rm C}$ signals from HP [1- $^{13}{\rm C}$]pyruvate and thermal signal reference [1- $^{13}{\rm C}$]acetate, respectively, $C_{\rm REF}$ and $C_{\rm HP}$ are concentrations of thermal signal reference [1- $^{13}{\rm C}$]acetate (4 M) and HP [1- $^{13}{\rm C}$]pyruvate, respectively, and $A_{\rm REF}$ and $A_{\rm HP}$ are effective cross sections of the NMR tubes for thermal signal reference [1- $^{13}{\rm C}$]acetate and HP [1- $^{13}{\rm C}$]pyruvate samples, respectively.

■ RESULTS AND DISCUSSION

Parahydrogen Enrichment. Three identical copies of the generator were employed for quality assurance prior to catalyst activation. Under conditions of liquid N₂ and 150 sccm p-H₂ flow rate, the benchtop NMR quantification yielded the following p-H₂ enrichment fractions: 48.4 ± 0.5 , 48.1 ± 0.5 , and $48.2 \pm 0.5\%$, demonstrating the robustness of the design in the context of reproducible generator construction. A representative NMR quantification of the p-H₂ fraction at 150 sccm flow rate is shown in Figure 3a. The remaining p-H₂ quantification studies were performed with one of the three devices. The flow rate was then varied from 150 to 1000 sccm (Figure 3b, blue bars) clearly demonstrating the reduction of the p-H₂ fraction with increased flow rate. This finding is rationalized as follows: the nonactivated catalyst has some potency for ortho ↔ para conversion, which is sufficient for slow-flowing H₂ gas. When the flow rate is fast (i.e., 1000 sccm), the slow ortho ↔ para conversion rate is no longer sufficient to allow the system to reach an equilibrium conversion while the gas moves along the catalyst-filled copper spiral, thus yielding a lower than expected p-H₂ fraction.

Catalyst Activation by Heating under H₂ Atmosphere. After catalyst activation in the copper spiral as described above, the performance of the same generator was evaluated at various flow rates (Figure 3b, red bars). The results clearly indicate that catalyst activation is indeed important in order to maximize the ortho ↔ para conversion, allowing the system to achieve full conversion at high flow rates up to 1,000 sccm. Although higher hydrogen flow rates were not tested due to limitations of the MFC, we expect the generator to perform well at substantially higher flow rates of at least 4000 sccm. Our expectation is based on the performance of a recently published cryogenic design, which employs catalyst-filled copper tubing filled with half the quantity of the catalyst (10 g vs 21 g employed here) in smaller ID/OD copper tubing.⁶⁴ This recently published design performed well at flow rates of up to 4000 sccm.⁶⁴

Utility of the Parahydrogen Generator for 13 C SABRE–SHEATH Hyperpolarization. Hyperpolarization of $[1^{-13}C]$ pyruvate was evaluated using another copy of the generator at a different site. It was employed for SABRE hyperpolarization studies of $[1^{-13}C]$ pyruvate using SABRE–SHEATH. The simultaneous exchange of p-H₂ and $[1^{-13}C]$ -pyruvate on the activated Ir-IMes catalyst leads to a buildup of ^{13}C hyperpolarization, as shown in Figure 4a. Figure 4b shows a representative spectrum of ^{13}C -hyperpolarized $[1^{-13}C]$ -pyruvate with signal enhancement ε of over 14,000-fold, corresponding to P_{13C} of 1.2% obtained via comparison of the NMR signal intensity with a reference sample, as shown in Figure 4c.

If near 100% p-H₂ would have been employed, P_{13C} would be tripled to P_{13C} = 3.5%. We note that P_{13C} strongly

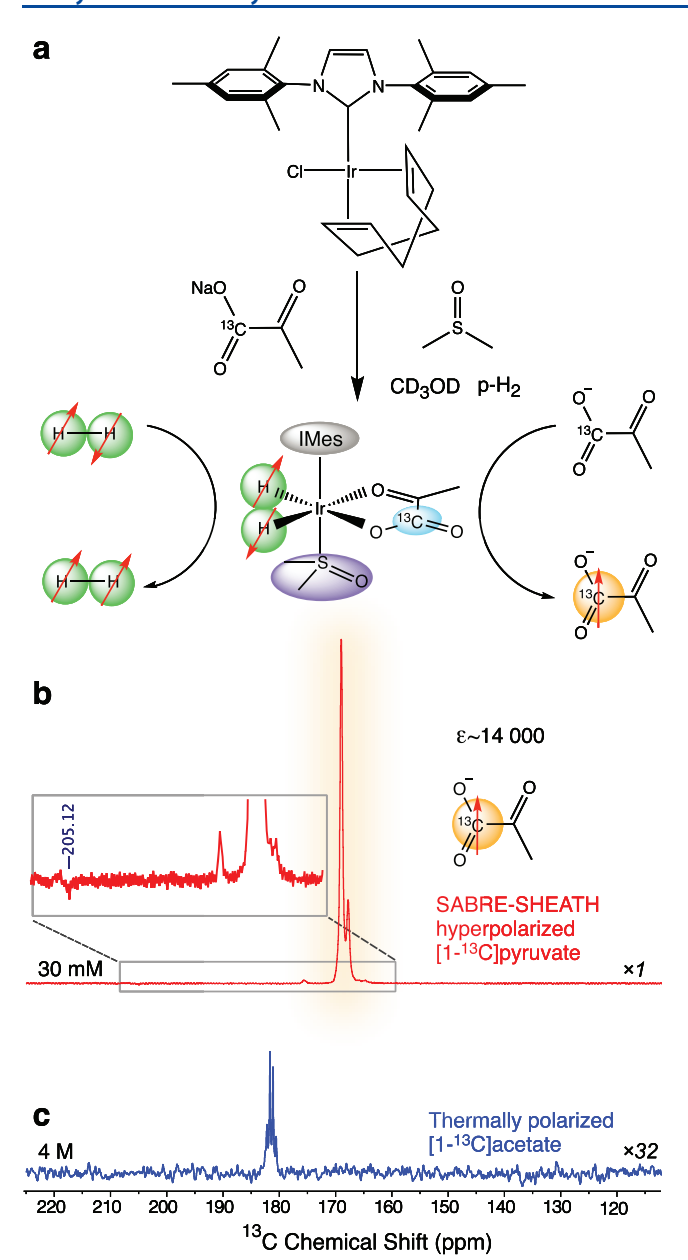


Figure 4. (a) Schematic of the catalytic system for SABRE–SHEATH hyperpolarization. The activated Ir complex catalyst, $[Ir(H_2)(\eta^2-pyruvate)(DMSO)$ (IMes)], transfers magnetization from p-H₂ to $[1^{-13}C]$ pyruvate through a J-coupled spin network. Both p-H₂ and pyruvate have weak, transient binding to the iridium complex. (b) Single-scan HP ^{13}C spectrum selected from SABRE–SHEATH experiments; enhancement $\varepsilon \approx 14,000$. Sample: 30 mM sodium $[1^{-13}C]$ pyruvate, 20 mM DMSO, and 7.8 mM Ir-IMes catalyst in methanol- d_4 ; the spectrum was acquired immediately following manual sample transfer to 1 T after 55 s p-H₂ bubbling at $B_T = -0.7 \ \mu T$. The inset of (b) shows a close-up of the ^{13}C spectrum. (c) Single-scan thermally polarized ^{13}C signal from 4 M sodium $[1^{-13}C]$ acetate using similar acquisition parameters. All experiments were performed with p-H₂ (~50% para-) at 1.0 T and overpressure (Magritek SpinSolve ^{13}C).

depends on the experimental conditions. To the best of our knowledge, the extrapolated $P_{\rm 13C}$ value reported here exceeds the highest reported value ($P_{\rm 13C}$ of 1.0% for [1-¹³C]pyruvate and $P_{\rm 13C}$ of 1.85% for [1,2-¹³C]pyruvate^{74,77} by threefold and nearly twofold respectively), representing a substantial

advancement for HP [1-¹³C]pyruvate production via the SABRE–SHEATH technique.

The pilot optimization of ¹³C SABRE-SHEATH conditions reveal ¹³C signal dependence on the microtesla magnetic field (Figure 5a), temperature (Figure 5b), polarization buildup

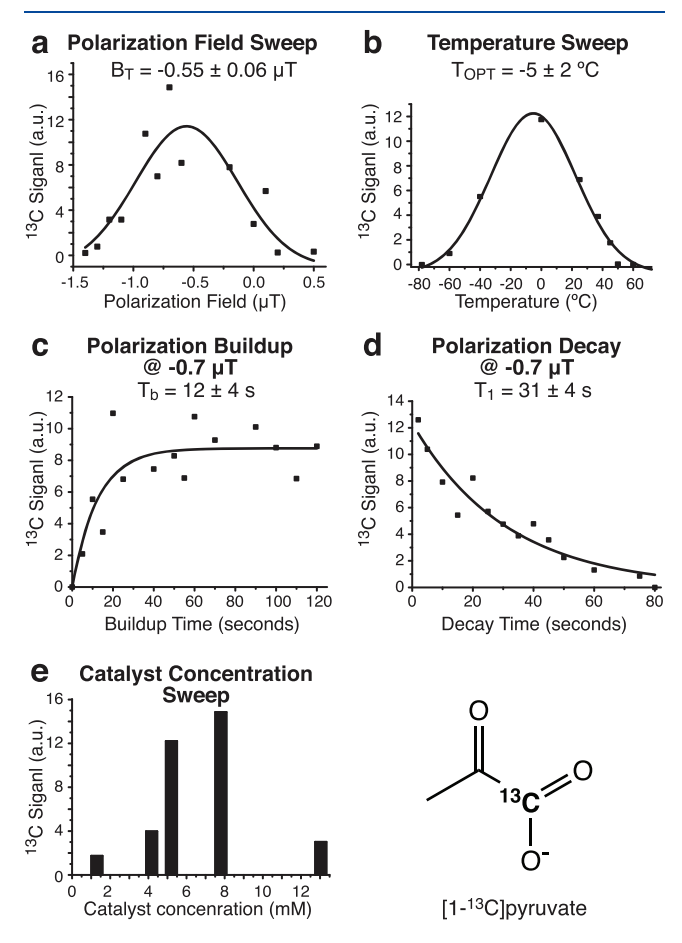


Figure 5. Pilot optimization of SABRE-SHEATH hyperpolarization of [1-13C]pyruvate: (a) magnetic field sweep of a sample of [Ir(COD)(IMes)] (13 mM) with sodium $[1-^{13}C]$ pyruvate (90 mM) and DMSO (120 mM) in 0.6 mL of methanol- d_4 at room temperature; (b) temperature sweep of a sample of [Ir(COD)-(IMes)] (7.8 mM) with sodium [1-13C]pyruvate (30 mM) and DMSO (20 mM) in 0.6 mL of methanol- d_4 at $B_T = -0.7 \mu T$; (c) p-H₂ bubbling duration sweep using a sample of [Ir(COD)(IMes)] (7.8 mM) with sodium [1-13C]pyruvate (30 mM) and DMSO (20 mM) in 0.6 mL of methanol- d_4 at $B_T = -0.7 \mu T$; (d) in-shield ¹³C T_1 signal decay using a sample of [Ir(COD)(IMes)] (7.8 mM) with sodium [1-13C]pyruvate (30 mM) and DMSO (20 mM) in 0.6 mL of methanol- d_4 at $B_T = -0.7 \mu T$; and (e) SABRE catalyst concentration sweep using samples of 30 mM sodium [1-13C]pyruvate and 20 mM DMSO in 0.6 mL of methanol- d_4 at $B_{\rm T}=-0.7~\mu{\rm T}$. All experiments were performed with 100 PSI p-H₂ (~50% para-) overpressure at ~100 sccm flow rate at 1.0 T (Magritek SpinSolve ¹³C).

time (i.e., the duration of p-H₂ bubbling, Figure 5c), and catalyst concentration (Figure 5e). The 13 C T_1 in-shield relaxation value of 31 \pm 4 s at [catalyst] = 7.8 mM is substantially longer than 15 N T_1 of ca. 12–15 s of [15 N₃]metronidazole at [catalyst]~2 mM 78 despite the fact that the 13 C gyromagnetic ratio is 2.5 times greater than that of the 15 N one; and therefore, the 13 C spin would be more prone to the catalyst-induced relaxation. We rationalize this observation by the greater distance of the 13 C1 nucleus from

Ir due to the presence of bridging oxygen (i.e., Ir-O= 13 C) versus direct Ir interaction with the 15 N nucleus (i.e., Ir $^{-15}$ N). This observation is important because longer in-shield 13 C T_1 at the microtesla magnetic field effectively results in greater P_{13} C.

We envision that additional future improvements for ¹³C pyruvate polarization can be made through the increase of p-H₂ pressure and flow rate⁷⁹ and the use of recently reported hardware for more precise calibration of the in-shield nanotesla magnetic field.⁸⁰

The reported results clearly demonstrate the utility of our generator to produce a HP state that can be easily detectable, even when using a benchtop NMR spectrometer operating at 1 T. We note that although [1-13C]-labeled pyruvate was employed, the resonance at 205 ppm corresponds to the natural ¹³C abundance signal from ¹³C2 locked in a singlet state with ¹³C1.⁷⁷ Thus, we anticipate that our generator can enable a wide range of p-H₂-based hyperpolarization studies in the context of development, optimization, and quality assurance of HP ¹³C compounds and biocompatible contrast agents even at the natural abundance 13C level. We also anticipate that other nuclei (15N, 19F, 1H, etc.) can also be readily studied using our low-cost and easy-to-maintain p-H₂ generator in combination with a benchtop NMR spectrometer. Such a combination should provide a straightforward gateway for HP studies with p-H₂ for a wide range of laboratories.

CONCLUSIONS

In summary, we report a robust design of a p-H₂ generator developed for operation at liquid N2 temperature based on many years of experience in our laboratories. We employed near real-time benchtop NMR spectroscopy for quantification of the p-H₂ fraction, indicating p-H₂ enrichment of ~48% (three separately constructed devices) at flow rates of up to 1000 sccm; moreover, it is expected that flow rates of up to 4000 sccm should be attainable without performance loss. Catalyst activation by heat under the H2 atmosphere was shown to be important for efficient operation at high flow rates. The utility of the generator has been investigated for SABRE-SHEATH ¹³C-hyperpolarization of [1-¹³C]pyruvate, the leading metabolic ¹³C contrast agent under investigation in clinical trials. Despite the low p-H2 fraction resulting in ~threefold signal reduction (vs near 100% p-H₂), it was possible to successfully hyperpolarize [1-13C]pyruvate for detection using a 1 T benchtop NMR spectrometer ($\varepsilon \approx$ 14,000, $P_{13C} \approx 1.2\%$). We anticipate that the reported generator design will be useful for those working on the development of p-H2-based hyperpolarization technologies (e.g., PHIP and SABRE), and particularly those working on developing new biocompatible compounds that can be employed as exogenous HP contrast agents. Taken together, the combination of the described p-H₂ generator and a benchtop NMR spectrometer embodies a low-cost and robust gateway to the field of p-H₂ hyperpolarization without substantial investment in complex infrastructure. Although on-demand p-H2 production for utility in SABRE hyperpolarization was demonstrated here, the produced p-H₂ gas can also be stored in an aluminum tank for weeks because p-H₂ back conversion to normal hydrogen is slow.^{36,64}

AUTHOR INFORMATION

Corresponding Author

Eduard Y. Chekmenev — Department of Chemistry, Integrative Biosciences (Ibio), Wayne State University, Karmanos Cancer Institute (KCI), Detroit, Michigan 48202, United States; Russian Academy of Sciences, Moscow 119991, Russia; Orcid.org/0000-0002-8745-8801; Email: chekmenevlab@gmail.com

Authors

Benjamin Chapman – Department of Materials and Metallurgical Engineering, South Dakota School of Mines and Technology, Rapid City, South Dakota 57701, United States

Baptiste Joalland – Department of Chemistry, Integrative Biosciences (Ibio), Wayne State University, Karmanos Cancer Institute (KCI), Detroit, Michigan 48202, United States; orcid.org/0000-0003-4116-6122

Collier Meersman – Department of Chemistry, Biology, and Health Sciences, South Dakota School of Mines and Technology, Rapid City, South Dakota 57701, United States

Jessica Ettedgui – Chemistry and Synthesis Center, National Heart, Lung, and Blood Institute, Bethesda, Maryland 20850, United States

Rolf E. Swenson – Chemistry and Synthesis Center, National Heart, Lung, and Blood Institute, Bethesda, Maryland 20850, United States

Murali C. Krishna — Center for Cancer Research, National Cancer Institute, National Institutes of Health, Bethesda, Maryland 20814, United States

Panayiotis Nikolaou — XeUS Technologies Limited, Lakatamia 2312, Nicosia, Cyprus; orcid.org/0000-0002-3802-0803

Kirill V. Kovtunov – International Tomography Center, SB RAS, Novosibirsk 630090, Russia; Novosibirsk State University, Novosibirsk 630090, Russia; orcid.org/0000-0001-7577-9619

Oleg G. Salnikov — International Tomography Center, SB RAS, Novosibirsk 630090, Russia; Novosibirsk State University, Novosibirsk 630090, Russia; Boreskov Institute of Catalysis SB RAS, Novosibirsk 630090, Russia; orcid.org/0000-0003-2266-7335

Igor V. Koptyug — International Tomography Center, SB RAS, Novosibirsk 630090, Russia; ⊙ orcid.org/0000-0003-3480-7649

Max E. Gemeinhardt – Department of Chemistry and Biochemistry, Southern Illinois University, Carbondale, Illinois 62901, United States

Boyd M. Goodson – Department of Chemistry and Biochemistry and Materials Technology Center, Southern Illinois University, Carbondale, Illinois 62901, United States; orcid.org/0000-0001-6079-5077

Roman V. Shchepin – Department of Chemistry, Biology, and Health Sciences, South Dakota School of Mines and Technology, Rapid City, South Dakota 57701, United States

Complete contact information is available at: https://pubs.acs.org/10.1021/acs.analchem.1c00716

Notes

The authors declare the following competing financial interest(s): EYC, PN, and BMG declare a stake of ownership in XeUS Technologies, LTD.

ACKNOWLEDGMENTS

We acknowledge Molecular Products Inc. for providing Ionex—Type O-P Catalyst. This work was supported by NSF CHE-1416268, CHE-1416432, CHE-1905341, and CHE-1904780, DOD CDMRP W81XWH-15-1-0271, W81XWH-15-1-0272, W81XWH-20-10576, and W81XWH-20-10578, NCI 1R21CA220137, NIBIB 1R01EB029829, and NHLBI 1R21HL154032. This project is funded in whole or in part with federal funds from the National Cancer Institute, National Institutes of Health, under contract no. HHSN261200800001E. B.M.G. acknowledges the support from a Cottrell Scholar SEED Award from Research Corporation for Science Advancement. I.V.K. and O.G.S. acknowledge financial support of this research by the Ministry of Science and Higher Education of the Russian Federation (grant no. 075-15-2020-779).

REFERENCES

- (1) Nikolaou, P.; Goodson, B. M.; Chekmenev, E. Y. Chem.—Eur. J. **2015**, 21, 3156–3166.
- (2) Goodson, B. M.; Whiting, N.; Coffey, A. M.; Nikolaou, P.; Shi, F.; Gust, B. M.; Gemeinhardt, M. E.; Shchepin, R. V.; Skinner, J. G.; Birchall, J. R.; Barlow, M. J.; Chekmenev, E. Y. *Emagres* **2015**, *4*, 797–810.
- (3) Ardenkjaer-Larsen, J. H.; Fridlund, B.; Gram, A.; Hansson, G.; Hansson, L.; Lerche, M. H.; Servin, R.; Thaning, M.; Golman, K. *Proc. Natl. Acad. Sci. U.S.A.* **2003**, *100*, 10158–10163.
- (4) Ardenkjaer-Larsen, J. H. J. Magn. Reson. 2016, 264, 3-12.
- (5) Golman, K.; Axelsson, O.; Jóhannesson, H.; Månsson, S.; Olofsson, C.; Petersson, J. S. Magn. Reson. Med. 2001, 46, 1-5.
- (6) Golman, K.; Ardenkjaer-Larsen, J. H.; Petersson, J. S.; Månsson, S.; Leunbach, I. Proc. Natl. Acad. Sci. U.S.A. 2003, 100, 10435–10439.
- (7) Golman, K.; in 't Zandt, R.; Thaning, M. Proc. Natl. Acad. Sci. U.S.A. 2006, 103, 11270–11275.
- (8) Mugler, J. P.; Altes, T. A. J. Magn. Reson. Imag. 2013, 37, 313-331.
- (9) Kovtunov, K. V.; Pokochueva, E. V.; Salnikov, O. G.; Cousin, S. F.; Kurzbach, D.; Vuichoud, B.; Jannin, S.; Chekmenev, E. Y.; Goodson, B. M.; Barskiy, D. A.; Koptyug, I. V. *Chem.—Asian J.* **2018**, 13, 1857—1871.
- (10) Rayner, P. J.; Duckett, S. B. Angew. Chem., Int. Ed. 2018, 57, 6742-6753.
- (11) Brindle, K. M. J. Am. Chem. Soc. 2015, 137, 6418-6427.
- (12) Kurhanewicz, J.; Vigneron, D. B.; Brindle, K.; Chekmenev, E. Y.; Comment, A.; Cunningham, C. H.; DeBerardinis, R. J.; Green, G. G.; Leach, M. O.; Rajan, S. S.; Rizi, R. R.; Ross, B. D.; Warren, W. S.; Malloy, C. R. *Neoplasia* **2011**, *13*, 81–97.
- (13) Nelson, S. J.; Kurhanewicz, J.; Vigneron, D. B.; Larson, P. E. Z.; Harzstark, A. L.; Ferrone, M.; van Criekinge, M.; Chang, J. W.; Bok, R.; Park, I.; Reed, G.; Carvajal, L.; Small, E. J.; Munster, P.; Weinberg, V. K.; Ardenkjaer-Larsen, J. H.; Chen, A. P.; Hurd, R. E.; Odegardstuen, L.-I.; Robb, F. J.; Tropp, J.; Murray, J. A. Sci. Transl. Med. 2013, 5, 198ra108.
- (14) Kurhanewicz, J.; Vigneron, D. B.; Ardenkjaer-Larsen, J. H.; Bankson, J. A.; Brindle, K.; Cunningham, C. H.; Gallagher, F. A.; Keshari, K. R.; Kjaer, A.; Laustsen, C.; Mankoff, D. A.; Merritt, M. E.; Nelson, S. J.; Pauly, J. M.; Lee, P.; Ronen, S.; Tyler, D. J.; Rajan, S. S.; Spielman, D. M.; Wald, L.; Zhang, X.; Malloy, C. R.; Rizi, R. *Neoplasia* **2019**, *21*, 1–16.
- (15) Bowers, C. R.; Weitekamp, D. P. Phys. Rev. Lett. 1986, 57, 2645-2648
- (16) Eisenschmid, T. C.; Kirss, R. U.; Deutsch, P. P.; Hommeltoft, S. I.; Eisenberg, R.; Bargon, J.; Lawler, R. G.; Balch, A. L. *J. Am. Chem. Soc.* 1987, 109, 8089–8091.
- (17) Bowers, C. R.; Weitekamp, D. P. J. Am. Chem. Soc. 1987, 109, 5541–5542.

- (18) Koptyug, I. V.; Kovtunov, K. V.; Burt, S. R.; Anwar, M. S.; Hilty, C.; Han, S.-I.; Pines, A.; Sagdeev, R. Z. J. Am. Chem. Soc. 2007, 129, 5580–5586.
- (19) Adams, R. W.; Aguilar, J. A.; Atkinson, K. D.; Cowley, M. J.; Elliott, P. I. P.; Duckett, S. B.; Green, G. G. R.; Khazal, I. G.; Lopez-Serrano, J.; Williamson, D. C. Science 2009, 323, 1708–1711.
- (20) Adams, R. W.; Duckett, S. B.; Green, R. A.; Williamson, D. C.; Green, G. G. R. *J. Chem. Phys.* **2009**, *131*, 194505.
- (21) Cowley, M. J.; Adams, R. W.; Atkinson, K. D.; Cockett, M. C. R.; Duckett, S. B.; Green, G. G. R.; Lohman, J. A. B.; Kerssebaum, R.; Kilgour, D.; Mewis, R. E. *J. Am. Chem. Soc.* **2011**, *133*, 6134–6137.
- (22) Muhammad, S. R.; Greer, R. B.; Ramirez, S. B.; Goodson, B. M.; Fout, A. R. ACS Catal. 2021, 11, 2011–2020.
- (23) Goldman, M.; Jóhannesson, H.; Axelsson, O.; Karlsson, M. Magn. Reson. Imag. 2005, 23, 153-157.
- (24) Goldman, M.; Johannesson, H.; Axelsson, O.; Karlsson, M. Compt. Rendus Chem. 2006, 9, 357-363.
- (25) Bhattacharya, P.; Chekmenev, E. Y.; Perman, W. H.; Harris, K. C.; Lin, A. P.; Norton, V. A.; Tan, C. T.; Ross, B. D.; Weitekamp, D. P. J. Magn. Reson. **2007**, 186, 150–155.
- (26) Hövener, J.-B.; Chekmenev, E. Y.; Harris, K. C.; Perman, W. H.; Robertson, L. W.; Ross, B. D.; Bhattacharya, P. Magn. Reson. Mater. Phys., Biol. Med. 2009, 22, 111–121.
- (27) Bhattacharya, P.; Chekmenev, E. Y.; Reynolds, W. F.; Wagner, S.; Zacharias, N.; Chan, H. R.; Bünger, R.; Ross, B. D. *NMR Biomed.* **2011**, 24, 1023–1028.
- (28) Perman, W. H.; Bhattacharya, P.; Leupold, J.; Lin, A. P.; Harris, K. C.; Norton, V. A.; Hoevener, J.-B.; Ross, B. D. *Magn. Reson. Imag.* **2010**, 28, 459–465.
- (29) Kadlecek, S.; Vahdat, V.; Nakayama, T.; Ng, D.; Emami, K.; Rizi, R. NMR Biomed. **2011**, 24, 933–942.
- (30) Hövener, J.-B.; Pravdivtsev, A. N.; Kidd, B.; Bowers, C. R.; Glöggler, S.; Kovtunov, K. V.; Plaumann, M.; Katz-Brull, R.; Buckenmaier, K.; Jerschow, A.; Reineri, F.; Theis, T.; Shchepin, R. V.; Wagner, S.; Bhattacharya, P.; Zacharias, N. M.; Chekmenev, E. Y. *Angew. Chem., Int. Ed.* **2018**, *57*, 11140–11162.
- (31) Kovtunov, K. V.; Koptyug, I. V.; Fekete, M.; Duckett, S. B.; Theis, T.; Joalland, B.; Chekmenev, E. Y. *Angew. Chem., Int. Ed.* **2020**, 59, 17788–17797.
- (32) Green, R. A.; Adams, R. W.; Duckett, S. B.; Mewis, R. E.; Williamson, D. C.; Green, G. G. R. Prog. Nucl. Magn. Reson. Spectrosc. 2012. 67, 1–48.
- (33) Kovtunov, K. V.; Zhivonitko, V. V.; Skovpin, I. V.; Barskiy, D. A.; Koptyug, I. V. *Top. Curr. Chem.* **2013**, 338, 123–180.
- (34) Hövener, J.-B.; Bär, S.; Leupold, J.; Jenne, K.; Leibfritz, D.; Hennig, J.; Duckett, S. B.; von Elverfeldt, D. NMR Biomed. **2013**, 26, 124–131.
- (35) Tom, B. A.; Bhasker, S.; Miyamoto, Y.; Momose, T.; McCall, B. J. Rev. Sci. Instrum. **2009**, 80, 016108.
- (36) Feng, B.; Coffey, A. M.; Colon, R. D.; Chekmenev, E. Y.; Waddell, K. W. J. Magn. Reson. 2012, 214, 258–262.
- (37) Birchall, J. R.; Coffey, A. M.; Goodson, B. M.; Chekmenev, E. Y. Anal. Chem. **2020**, 92, 15280–15284.
- (38) Gamliel, A.; Allouche-Arnon, H.; Nalbandian, R.; Barzilay, C. M.; Gomori, J. M.; Katz-Brull, R. *Appl. Magn. Reson.* **2010**, *39*, 329–345.
- (39) Farkas, A. Orthohydrogen, Parahydrogen, and Heavy Hydrogen; Cambridge University Press: Cambridge, 1935.
- (40) Bowers, C. R. Sensitivity Enhancement Utilizing Parahydrogen. *eMagRes*; John Wiley & Sons, Ltd, 2007.
- (41) Goldman, M.; Johannesson, H. Compt. Rendus Chem. 2005, 6, 575-581.
- (42) Kadlecek, S.; Emami, K.; Ishii, M.; Rizi, R. J. Magn. Reson. 2010, 205, 9–13.
- (43) Bär, S.; Lange, T.; Leibfritz, D.; Hennig, J.; von Elverfeldt, D.; Hoevener, J.-B. *J. Magn. Reson.* **2012**, 225, 25–35.
- (44) Cai, C.; Coffey, A. M.; Shchepin, R. V.; Chekmenev, E. Y.; Waddell, K. W. J. Phys. Chem. B 2013, 117, 1219–1224.

- (45) Barskiy, D. A.; Shchepin, R. V.; Tanner, C. P. N.; Colell, J. F. P.; Goodson, B. M.; Theis, T.; Warren, W. S.; Chekmenev, E. Y. ChemPhysChem 2017, 18, 1493–1498.
- (46) Bales, L. B.; Kovtunov, K. V.; Barskiy, D. A.; Shchepin, R. V.; Coffey, A. M.; Kovtunova, L. M.; Bukhtiyarov, A. V.; Feldman, M. A.; Bukhtiyarov, V. I.; Chekmenev, E. Y.; Koptyug, I. V.; Goodson, B. M. J. Phys. Chem. C 2017, 121, 15304—15309.
- (47) Theis, T.; Truong, M. L.; Coffey, A. M.; Shchepin, R. V.; Waddell, K. W.; Shi, F.; Goodson, B. M.; Warren, W. S.; Chekmenev, E. Y. J. Am. Chem. Soc. 2015, 137, 1404–1407.
- (48) Truong, M. L.; Theis, T.; Coffey, A. M.; Shchepin, R. V.; Waddell, K. W.; Shi, F.; Goodson, B. M.; Warren, W. S.; Chekmenev, E. Y. I. Phys. Chem. C 2015, 119, 8786–8797.
- (49) Zhivonitko, V. V.; Skovpin, I. V.; Koptyug, I. V. Chem. Commun. 2015, 51, 2506–2509.
- (50) Shchepin, R. V.; Goodson, B. M.; Theis, T.; Warren, W. S.; Chekmenev, E. Y. ChemPhysChem **2017**, *18*, 1961–1965.
- (51) Plaumann, M.; Bommerich, U.; Trantzschel, T.; Lego, D.; Dillenberger, S.; Sauer, G.; Bargon, J.; Buntkowsky, G.; Bernarding, J. *Chem.—Eur. J.* **2013**, *19*, 6334–6339.
- (52) Olaru, A. M.; Burt, A.; Rayner, P. J.; Hart, S. J.; Whitwood, A. C.; Green, G. G. R.; Duckett, S. B. *Chem. Commun.* **2016**, *52*, 14482–14485.
- (53) Rayner, P. J.; Burns, M. J.; Olaru, A. M.; Norcott, P.; Fekete, M.; Green, G. G. R.; Highton, L. A. R.; Mewis, R. E.; Duckett, S. B. *Proc. Natl. Acad. Sci. U.S.A.* **2017**, *114*, E3188–E3194.
- (54) Fekete, M.; Ahwal, F.; Duckett, S. B. J. Phys. Chem. B 2020, 124, 4573-4580.
- (55) Korchak, S.; Mamone, S.; Glöggler, S. ChemistryOpen 2018, 7, 672–676.
- (56) Shchepin, R. V.; Birchall, J. R.; Chukanov, N. V.; Kovtunov, K. V.; Koptyug, I. V.; Theis, T.; Warren, W. S.; Gelovani, J. G.; Goodson, B. M.; Shokouhi, S.; Rosen, M. S.; Yen, Y.-F.; Pham, W.; Chekmenev, E. Y. Chem.—Eur. J. 2019, 25, 8829–8836.
- (57) Reineri, F.; Boi, T.; Aime, S. Nat. Commun. 2015, 6, 5858.
- (58) Hövener, J.-B.; Chekmenev, E. Y.; Harris, K. C.; Perman, W. H.; Tran, T. T.; Ross, B. D.; Bhattacharya, P. Magn. Reson. Mater. Phys., Biol. Med. 2009, 22, 123–134.
- (59) Bhattacharya, P.; Harris, K.; Lin, A. P.; Mansson, M.; Norton, V. A.; Perman, W. H.; Weitekamp, D. P.; Ross, B. D. Magn. Reson. Mater. Phys., Biol. Med. 2005, 18, 245–256.
- (60) Tam, S.; Fajardo, M. E. Rev. Sci. Instrum. 1999, 70, 1926-1932.
- (61) Knopp, G.; Kirch, K.; Beaud, P.; Mishima, K.; Spitzer, H.; Radi, P.; Tulej, M.; Gerber, T. *J. Raman Spectrosc.* **2003**, *34*, 989–993.
- (62) Parrott, A. J.; Dallin, P.; Andrews, J.; Richardson, P. M.; Semenova, O.; Halse, M. E.; Duckett, S. B.; Nordon, A. Appl. Spectrosc. 2019, 73, 88–97.
- (63) Du, Y.; Zhou, R.; Ferrer, M.-J.; Chen, M.; Graham, J.; Malphurs, B.; Labbe, G.; Huang, W.; Bowers, C. R. J. Magn. Reson. **2020**, 321, 106869.
- (64) Nantogma, S.; Joalland, B.; Wilkens, K.; Chekmenev, E. Y. *Anal. Chem.* **2021**, 93, 3594–3601.
- (65) Semenova, O.; Richardson, P. M.; Parrott, A. J.; Nordon, A.; Halse, M. E.; Duckett, S. B. *Anal. Chem.* **2019**, *91*, 6695–6701.
- (66) Joalland, B.; Schmidt, A. B.; Kabir, M. S. H.; Chukanov, N. V.; Kovtunov, K. V.; Koptyug, I. V.; Hennig, J.; Hövener, J.-B.; Chekmenev, E. Y. *Anal. Chem.* **2020**, 92, 1340–1345.
- (67) Chae, H.; Min, S.; Jeong, H. J.; Namgoong, S. K.; Oh, S.; Kim, K.; Jeong, K. Anal. Chem. **2020**, 92, 10902–10907.
- (68) Zacharias, N. M.; McCullough, C. R.; Wagner, S.; Sailasuta, N.; Chan, H. R.; Lee, Y.; Hu, J.; Perman, W. H.; Henneberg, C.; Ross, B. D.; Bhattacharya, P. J. Mol. Imag. Dynam. 2016, 6, 123.
- (69) Shchepin, R. V.; Barskiy, D. A.; Coffey, A. M.; Manzanera Esteve, I. V.; Chekmenev, E. Y. *Angew. Chem., Int. Ed.* **2016**, *55*, 6071–6074.
- (70) Reineri, F.; Viale, A.; Giovenzana, G.; Santelia, D.; Dastrù, W.; Gobetto, R.; Aime, S. *J. Am. Chem. Soc.* **2008**, *130*, 15047–15053.
- (71) Reineri, F.; Viale, A.; Dastrù, W.; Gobetto, R.; Aime, S. Contrast Media Mol. Imaging 2011, 6, 77–84.

- (72) Emmett, P. H.; Harkness, R. W. J. Am. Chem. Soc. 1935, 57, 1624–1631.
- (73) Das, T.; Kweon, S.-C.; Nah, I. W.; Karng, S. W.; Choi, J.-G.; Oh, I.-H. *Cryogenics* **2015**, *69*, 36–43.
- (74) Iali, W.; Roy, S. S.; Tickner, B. J.; Ahwal, F.; Kennerley, A. J.; Duckett, S. B. *Angew. Chem., Int. Ed.* **2019**, 58, 10271–10275.
- (75) Merritt, M. E.; Harrison, C.; Storey, C.; Jeffrey, F. M.; Sherry, A. D.; Malloy, C. R. *Proc. Natl. Acad. Sci. U.S.A.* **2007**, *104*, 19773–19777.
- (76) Gemeinhardt, M. E.; Limbach, M. N.; Gebhardt, T. R.; Eriksson, C. W.; Eriksson, S. L.; Lindale, J. R.; Goodson, E. A.; Warren, W. S.; Chekmenev, E. Y.; Goodson, B. M. *Angew. Chem., Int. Ed.* **2020**, *59*, 418–423.
- (77) Tickner, B. J.; Semenova, O.; Iali, W.; Rayner, P. J.; Whitwood, A. C.; Duckett, S. B. Catal. Sci. Technol. 2020, 10, 1343-1355.
- (78) Birchall, J. R.; Kabir, M. S. H.; Salnikov, O. G.; Chukanov, N. V.; Svyatova, A.; Kovtunov, K. V.; Koptyug, I. V.; Gelovani, J. G.; Goodson, B. M.; Pham, W.; Chekmenev, E. Y. *Chem. Commun.* **2020**, *56*, 9098–9101.
- (79) Salnikov, O. G.; Chukanov, N. V.; Svyatova, A.; Trofimov, I. A.; Kabir, M. S. H.; Gelovani, J. G.; Kovtunov, K. V.; Koptyug, I. V.; Chekmenev, E. Y. *Angew. Chem., Int. Ed.* **2021**, *60*, 2406–2413.
- (80) Joalland, B.; Nantogma, S.; Chowdhury, M. R. H.; Nikolaou, P.; Chekmenev, E. Y. Magn. Reson. Chem. 2021, DOI: 10.1002/mrc.5167.